

LIST: Learning to Index Spatio-Textual Data for Embedding based Spatial Keyword Queries

Ziqi Yin[†], Shanshan Feng[‡], Shang Liu[†], Gao Cong[†], Yew Soon Ong[†], Bin Cui^{*}

[†]Nanyang Technological University, Singapore

[‡]Centre for Frontier AI Research, A*STAR, Singapore; ^{*}Peking university, Beijing, China

{ziqi003@e., shang006@e., gaocong@, asysong@}ntu.edu.sg; victor_fengss@foxmail.com; bin.cui@pku.edu.cn

Abstract—With the proliferation of spatio-textual data, Top-k KNN spatial keyword queries (TkQs), which return a list of objects based on a ranking function that evaluates both spatial and textual relevance, have found many real-life applications. Existing geo-textual indexes for TkQs use traditional retrieval models like BM25 to compute text relevance and usually exploit a simple linear function to compute spatial relevance, but its effectiveness is limited. To improve effectiveness, several deep learning models have recently been proposed, but they suffer severe efficiency issues. To the best of our knowledge, there are no efficient indexes specifically designed to accelerate the top-k search process for these deep learning models.

To tackle these issues, we propose a novel technique, which Learns to Index the Spatio-Textual data for answering embedding based spatial keyword queries (called LIST). LIST is featured with two novel components. Firstly, we propose a lightweight and effective relevance model that is capable of learning both textual and spatial relevance. Secondly, we introduce a novel machine learning based Approximate Nearest Neighbor Search (ANNS) index, which utilizes a new learning-to-cluster technique to group relevant queries and objects together while separating irrelevant queries and objects. Two key challenges in building an effective and efficient index are the absence of high-quality labels and unbalanced clustering results. We develop a novel pseudo-label generation technique to address the two challenges. Experimental results show that LIST significantly outperforms state-of-the-art methods on effectiveness, with improvements up to 19.21% and 12.79% in terms of NDCG@1 and Recall@10, and is three orders of magnitude faster than the most effective baseline.

I. INTRODUCTION

With the proliferation of mobile Internet, spatio-textual (a.k.a geo-textual) data is being increasingly generated. Examples of spatio-textual data include (1) web pages with geographical information; (2) user-generated text content with location information, such as geo-tagged tweets and reviews related to local stores; (3) Points of Interest (POI) in local business websites or location-based apps [1]; (4) multimedia data containing both text and geo-locations, like photos shared on social platforms that provide both textual descriptions and geographic location. Meanwhile, with the prevalence of smartphones, accessing and querying spatio-textual data has become increasingly frequent. This trend calls for techniques to process spatial keyword queries efficiently and effectively, which take query keywords and location as input and return objects that match the given requirements. An example query is to retrieve geo-textual objects with texts relevant to the keywords ‘delicious Italian restaurants’ and located near the query’s location, and the result is a list of k geo-textual objects ranked by a relevance model considering both spatial and textual relevance.

Spatial keyword queries have applications in many scenarios such as geographic search engines, location-based services, and local web advertising tailored to specific regions. To meet diverse user needs, various spatial keyword queries have been introduced [2]–[4]. Among them, the Top-k KNN Spatial Keyword Query (TkQ) [2] retrieves top-k geo-textual objects based on a ranking function that evaluates both spatial and textual relevance. According to the experimental evaluation [5], TkQs return more relevant objects compared to several other spatial keyword queries like the Boolean KNN Query [4], which retrieves the geo-textual objects containing all the query keywords and rank them according to their spatial relevance (or proximity) to the query location. *Most of the existing studies on spatial keyword queries focus on the improvement in the efficiency of handling spatial keyword queries.* As such, many indexes [6] and corresponding query processing algorithms have been developed.

Motivations. The existing indexes [2], [7]–[9] designed for the TkQ query typically compute textual relevance using traditional retrieval models such as BM25 [10] and TF-IDF [11], which rely on exact word matching to evaluate textual relevance. These traditional models often suffer from the word mismatch issue, i.e., synonyms or paraphrases that consist of completely different tokens may convey the same meanings, which limits their effectiveness (as to be shown in Section III-B). For example, when a user searches for ‘nearby bar’, nearby bars named ‘pub’ or ‘tavern’ will be ignored by these traditional models, although they are relevant to the query.

As for spatial relevance, existing indexes [2], [7]–[9] for the TkQ query typically compute spatial relevance by a linear function of the distance between the query location and the location of a geo-textual object. The implicit assumption behind this practice is that the spatial preference for geo-textual objects is a linear function of distance. However, this assumption was not examined previously and we find it does not hold on our real-life datasets. From our dataset, we find that the spatial preference for geo-textual objects is not a linear function of distance, but exhibits a significant (non-linear) decrease with the increase of distance (detailed in Section III-B). This motivates us to design a more effective spatial relevance module. A straightforward approach would be to employ an exponential function. However, our experiments indicate that this method is even less effective compared to the linear function (shown in Section V-E).

To improve effectiveness, several deep learning based relevance models [5], [12], [13] propose to compute textual relevance based on word embeddings. For example, DrW [5]

employs embeddings generated from the Bert model, identifying top-k relevant terms from geo-textual object description for each query keyword based on the embeddings, and uses an attention mechanism to aggregate scores of each query keyword. Although these approaches could achieve better effectiveness, they have very high query latency for computing the relevance score since they rely on embeddings and neural networks (detailed in Section III-B). *To the best of our knowledge, there are no efficient indexes specifically designed to expedite the top-k search process for these deep relevance models.*

Existing geo-textual indexes are developed based on traditional retrieval models such as TF-IDF. For instance, IR-Tree [2] augments each R-Tree [14] node with a pseudo-inverted file including the words of all objects inside that node. These indexes cannot be used to handle embedding based spatial keyword queries, which represent the semantic meaning of query keywords with a high-dimensional embedding. Although Approximate Nearest Neighbor Search (ANNS) indexes [15]–[17] are designed for embedding retrieval, none of these ANNS indexes take into account the spatial factor, which is essential for spatial keyword queries. Directly using these ANNS indexes for spatial keyword queries results in severe degradation of effectiveness (as to be shown in Section V-B). It is an open problem to incorporate spatial factors into ANNS indexes to support embedding based spatial keyword queries.

Objectives. To address the aforementioned issues, this work aims to (1) design an embedding based lightweight yet effective spatio-textual relevance model as the ranking function, and (2) design a novel index to speed up high-dimensional embedding based spatial keyword queries.

To achieve the two objectives, we propose a novel solution, which learns to index spatio-textual data for answering embedding based spatial keyword queries. We denote this retriever by LIST, which is featured with two new components. First, LIST develops a lightweight and effective relevance model as the ranking function, which comprises three modules: a textual dual-encoder module, a novel learning based spatial relevance module, and a new weight learning module.

Second, LIST introduces a novel machine learning based ANNS index. For both embedding based spatial keyword queries and geo-textual objects, our proposed index utilizes the learning-to-cluster technique, which was developed for image clustering in the field of computer vision, to cluster relevant geo-textual objects and queries together and build an index. Existing learning-to-cluster techniques [18], [19] rely on partial pairwise similar/dis-similar relationships of images for training, where the pairwise labels are easy to obtain for images. However, such pairwise positive labels for queries and geo-textual objects in our problem are very sparse and high-quality negative labels are absent, which are important for learning-to-cluster. Additionally, when the number of clusters exceeds the number of image classes, the existing learning-to-cluster technique will produce a highly skewed cluster distribution [18], which will hurt the efficiency. To address these challenges, we propose a novel pseudo-negative label generation method, which employs the trained relevance model to produce high-quality pseudo-negative labels. These informative negative labels combined with ground-truth positive (relevant) labels (e.g., click-through or human annotation, detailed in Section V-A) enable our index to learn both spatial

and textual information, thereby clustering relevant objects and queries together while separating irrelevant objects and queries.

The contributions of this work are summarized as follows:

- **New Index.** We develop a novel machine learning based ANNS index that can speed up embedding based spatial keyword queries. Different from existing ANNS indexes, it extends the learning-to-cluster technique to cluster relevant objects and queries together. To build an effective and efficient index, we propose a novel pseudo-label generation approach. To the best of our knowledge, this is the first index tailored for embedding based spatial keyword queries. Additionally, this is the first geo-textual index to utilize a neural network for retrieval without relying on an explicit tree structure and associated heuristic algorithms.
- **New Relevance Model.** We develop a lightweight and effective relevance model. It is featured with a novel learning-based spatial relevance module to learn spatial relevance adaptively, a new weight learning mechanism to determine the weights between textual and spatial relevance, and a dual-encoder module to compute textual relevance.
- **Extensive Experiments.** We extensively evaluate the effectiveness and efficiency of our proposed LIST solution on three real-world datasets. Experimental results show that LIST outperforms the state-of-the-art baseline algorithms for effectiveness by an improvement up to 19.21% and 12.79% in terms of NDCG@1 and Recall@10 respectively and is three orders of magnitude faster than the most effective baseline. Our implementation is released at <https://github.com/Heisenberg-Yin/LIST>.

II. RELATED WORK

Spatio-Textual Relevance Models. Spatial keyword queries have attracted extensive attention and many types of spatial keyword queries [2]–[4] are proposed. Among them, Top-k KNN Spatial-Keyword Query (TkQ) [2] aims to retrieve top-k geo-textual objects based on a ranking function that evaluates both spatial relevance and text relevance. The earlier work [2] computes the textual relevance with traditional retrieval models like BM25 [10] and TF-IDF [11] and exploits a simple linear function for spatial relevance. However, these traditional methods have limited effectiveness.

To enhance the effectiveness, several deep learning based methods [5], [12], [13] have been developed for query-POI matching, which is essentially spatial keyword query. PALM [13] considers geographic information by using location embedding techniques and combines it with semantic representations for query-POI matching. DrW [5] computes the deep textual relevance on the term level of query and geo-textual objects and uses the attention mechanism to aggregate scores of each term for spatial keyword queries and design a learning-based method to learn a query-dependent weight to balance textual relevance and spatial relevance. MGeo [12] employs a geographic encoder and a multi-modal interaction module, treating geographic context as a new modality and using text information as another modality. MGeo aligns these two modalities into the same latent space and computes relevance scores based on the produced representations. However, these deep learning based methods focus on improving the effectiveness, but ignore the efficiency issue.

Spatio-Textual Indexes. Although various spatio-textual indexes [2]–[4], [7]–[9], [20]–[30] have been designed to efficiently answer spatial keyword queries, they are all designed for traditional retrieval models (e.g., TF-IDF), and are unsuitable for high-dimensional embedding based retrieval models used by deep learning based methods.

We are aware that several indexes [31], [32] have been introduced to incorporate semantic representations into the TkQ scheme. For example, S²R-Tree [32] projects the word embeddings to an m -dimensional vector using a pivot-based technique (m as low as 2). It employs R-trees to index objects based on their geo-locations and m -dimensional vectors hierarchically. When the dimensionality reaches hundreds, which are common for embeddings, such methods are no better than a linear scan due to the curse of dimensionality [33].

Different from previous spatio-textual indexes developed to accelerate the search for top-k objects with traditional relevance models (which is called sparse retrieval), we aim to design an index to accelerate the search for top-k objects with embedding based relevance models (which is called dense retrieval), which is still an open problem for geo-textual data.

Deep Textual Relevance Models and Approximate Nearest Neighbor Search Indexes. Our work is related to deep textual relevance models and the corresponding Approximate Nearest Neighbor Search (ANNS) index techniques. The deep textual relevance models can be broadly classified into two categories: interaction-focused models and representation-focused models [34]. The first category of models (e.g., ARC-II [35] and MatchPyramid [36]) calculates the word-level similarity between queries and documents for the final relevance scores. DrW [5] belongs to this category. Although this category of methods may have better effectiveness, these methods are usually computationally expensive. The second category of models (e.g., DSSM [37]) extracts global semantic representation for input text and uses functions like the inner product to compute the relevance score between representations. This category of models used to be less effective than the first category of models. However, with the emergence of the dual-encoder architecture [38], [39], which employs Pre-trained Large Language Models (PLMs) to extract global semantic representation, it has become a well-established paradigm in document retrieval [40]–[44]. For the second category of methods, to support efficient retrieval, the learned embeddings are usually indexed for Approximate Nearest Neighbor Search (ANNS) [34].

ANNS indexes are developed to expedite the top-k search on high-dimensional data. These techniques can be broadly categorized into two types. The first type focuses on searching a subset of database. The representative methods include inverted file index (IVF) based methods [45]–[47], hashing-based methods [48]–[51], and graph-based methods [17], [52]. These ANNS indexes rely on heuristic algorithms or centroids to find candidates. Specifically, Inverted File Index (IVF) [46] partitions data into clusters using the k-means algorithm and routes queries to clusters based on the query’s distance to the clusters’ centroids. Graph-based algorithms like Hierarchical Navigable Small World (HNSW) index [52] construct proximity graphs and perform a beam search on the graph for a given query to find similar embeddings. Hashing-based methods like Locality-Sensitive Hashing (LSH) index [53] generate top-k

candidates by hashing vectors into buckets and then retrieving the closest items from those buckets as candidates. The other type aims to accelerate the search process itself, such as quantization-based methods [46], [54], [54]–[56].

Our method belongs to the first category and is orthogonal to the second category. Our proposed index differs from previous ANNS indexes in two aspects: (1) Our proposed index is designed for embeddings based spatio-textual relevance models. In contrast, existing ANNS indexes are only for textual relevance. (2) Instead of using heuristic algorithms to generate candidates, our proposed index learns from query-object pairs in a data-driven manner and employs neural networks for data partitioning and query routing. Notably, our proposed index utilizes a novel learning-to-cluster technique to group geo-textual objects, while the IVF index employs the conventional k -means algorithm to cluster embeddings.

III. PROBLEM STATEMENT AND MOTIVATIONS

A. Preliminary

We consider a geo-textual object dataset D , where each geo-textual object $o \in D$ has a location description $o.loc$ and a textual document description $o.doc$. The location description $o.loc$ is a two-dimensional GPS coordinate composed of latitude and longitude. The document description $o.doc$ reflects the textual content. The Top-k KNN Spatial-Keyword Query (TkQ) [2] is defined as follows.

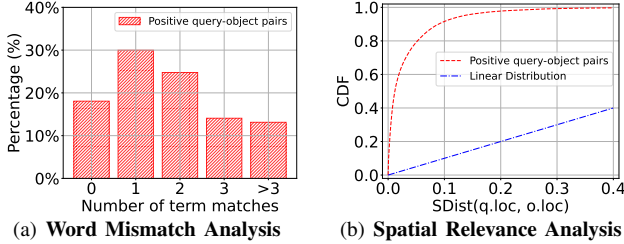
Top-k KNN Spatial-Keyword Query (TkQ): Given a query $q = \langle loc, doc, k \rangle$, where $q.doc$ denotes the query keywords, $q.loc$ is the query location, and $q.k$ is the number of returned objects, we aim to retrieve k objects with the highest relevance scores $ST(q, o)$:

$$ST(q, o) = (1 - \alpha) \times SRel(q.loc, o.loc) + \alpha \times TRel(q.doc, o.doc). \quad (1)$$

A higher score $ST(q, o)$ indicates higher relevance between the given query q and object o . Here, $SRel(q.loc, o.loc)$ denotes the spatial relevance between $q.loc$ and $o.loc$ and is often calculated by $1 - SDist(q.loc, o.loc)$, where $SDist(q.loc, o.loc)$ represents the spatial closeness and is usually computed by the normalized Euclidean distance: $SDist(q.loc, o.loc) = \frac{dist(q.loc, o.loc)}{dist_{max}}$, where $dist(q.loc, o.loc)$ denotes the Euclidean distance between $q.loc$ and $o.loc$ and $dist_{max}$ is the maximum distance between any two objects in the object dataset. Here, $TRel(q.doc, o.doc)$ denotes the text relevance between $p.doc$ and $q.doc$ and is computed by information retrieval models like BM25 [10], and then normalize to a scale similar to spatial relevance. Here, $\alpha \in [0, 1]$ is a weight parameter to balance the spatial and text relevance.

B. Data Analysis and Motivations

Word Mismatch. As discussed earlier, existing indexes [2], [7], [9] utilize traditional ranking methods, such as BM25 [10] and TF-IDF [11], to compute textual relevance. These models often suffer from the word mismatch issue, which reduces their effectiveness. As shown in Figure 1(a), in the Beijing dataset, nearly 20% of the ground-truth query-object positive (relevant) pairs have no overlap of words. Since these traditional models rely on exact word matching to compute text relevance, relevant objects may receive a low or even zero textual relevance from these models. For instance, given a



(a) **Word Mismatch Analysis** (b) **Spatial Relevance Analysis**

Fig. 1: Figure 1(a) shows the percentage distribution of ground-truth positive query-object pairs based on the number of matching terms on the Beijing dataset. Figure 1(b) compares the CDF of spatial distance for ground-truth positive query-object pairs and the linear distribution on the Beijing dataset. search ‘nearby drugstore’, if the search engine employs the BM25 to determine textual relevance, a drugstore labeled as ‘pharmacy’ would get a textual relevance score of zero.

Spatial Relevance. Previous studies [2], [5] typically compute spatial relevance by $1 - SDist(q.loc, o.loc)$. The implicit assumption for the linear formulation is that the user preference for geo-textual objects is a linear function of distance. However, this assumption was not examined previously and we found it does not really hold on our real-life datasets. In Figure 1(b), we illustrate this issue by comparing the cumulative distribution function (CDF) of ground-truth positive (relevant) query-object pairs with the ‘Linear Distribution’, a linearly ascending hypothetical scenario that positive query-object pairs are uniformly distributed across the range $[0, 1]$. This figure shows a sharp increase in the CDF of ground-truth positive pairs for $SDist(q.loc, o.loc)$ below 0.1, a pattern that greatly differs from the hypothetical scenario.

Efficiency. To address this issue, several recent studies [5], [13], [57] have utilized deep learning techniques to evaluate textual relevance, thereby enhancing ranking effectiveness. However, these methods rely on word embeddings and deep neural networks to compute textual relevance, resulting in high querying latency. For instance, DrW [5] needs to identify the top-k relevant words from each object for each query word, and then aggregate these word pairs using an attention mechanism to compute the textual relevance. On the Geo-Glue dataset, which comprises 2.8 million objects, DrW takes more than 7 seconds to answer a query on average in our experiment, which aligns with the results reported in [5]. This makes them unsuitable as a retriever for practical geo-textual object retrieval applications, although they can be used as rerankers for a small number of retrieved objects.

Incorporating deep textual relevance into spatial keyword queries has presented significant efficiency challenges. On the one hand, the index techniques developed for spatial keyword queries are designed based on the traditional retrieval models such as BM25 and cannot be used to handle embedding-based spatial keyword queries. On the other hand, existing ANNS indexes, which are discussed in Section II, do not consider spatial relevance. It is an open problem of incorporating spatial relevance into the ANNS indexes to support spatial keyword queries. Directly employing existing ANNS indexes for spatial keyword queries will result in severe degradation of effectiveness (shown in Section V-B).

C. Problem Statement

To address these issues, we aim to (1) design a lightweight and effective embedding-based spatio-textual relevance model

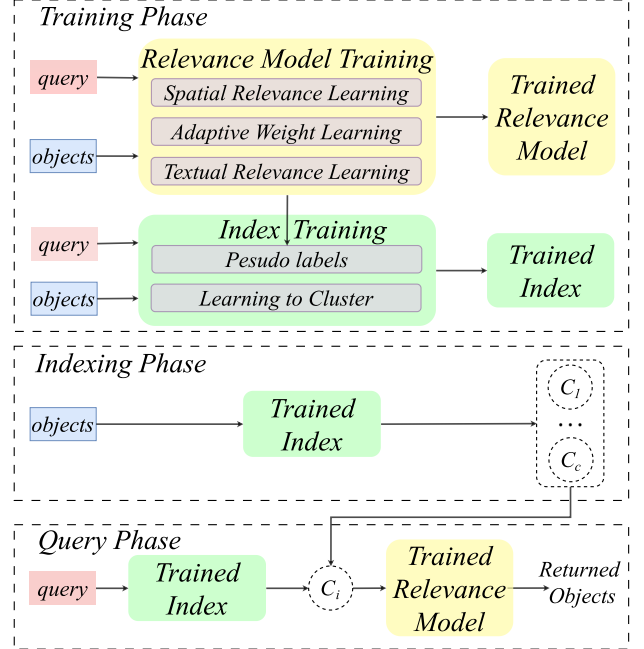


Fig. 2: The three phases of our retriever LIST: the training, indexing, and query phase. LIST consists of a relevance model (shown in yellow) and an index (shown in green).

as the ranking function, and (2) develop an index that can accelerate the top-k search process of embedding based spatial keyword queries.

IV. PROPOSED RETRIEVER (LIST)

A. Overview

As discussed in the introduction, LIST is featured with a novel machine learning based ANNS index and a new relevance model. Notably, our index is applicable to any textual relevance model that transforms query keywords and object text descriptions into two separate embeddings.

The workflow of LIST is illustrated in Figure 2, which has three phases: the training, indexing, and query phase. During the training phase, we first train our relevance model, and then train our index. During the indexing phase, each object is partitioned into one cluster. During the query phase, the trained index routes each query to a cluster or a subset of clusters that have the highest probabilities. In the cluster, LIST returns k objects with the highest scores ranked by the trained relevance model as the query result.

B. The Proposed Relevance Model

Textual Relevance Learning. Inspired by the dual-encoder model’s great success in document retrieval [38], we employ a dual-encoder module to encode both the query keywords and the document into two separate embeddings and calculate textual relevance using the two embeddings, which is used in spatial keyword query for the first time. Compared with previous relevance models [5] which rely on word embeddings and complex neural networks, this approach is more efficient.

This module comprises an object encoder E_o and a query encoder E_q , which are pre-trained language models like Bert [58]. The encoder takes the textual content of a query or object as input, captures interactions between terms by a transformer-based model, and finally utilizes the representation

of the [CLS] token as the global semantic representation, which is a d -dimensional dense vector. This process is formulated as:

$$\begin{aligned} o.emb &= E_o(o.doc; \theta_o), o.emb \in \mathbb{R}^d, \\ q.emb &= E_q(q.doc; \theta_q), q.emb \in \mathbb{R}^d. \end{aligned} \quad (2)$$

where $E_o(\cdot; \theta_o)$ denotes the object encoder parameterized with θ_o and $E_q(\cdot; \theta_q)$ denotes the query encoder parameterized with θ_q . Then the text relevance score can be calculated by the inner product between the $q.emb$ and $o.emb$,

$$TRel(q.doc, o.doc) = q.emb \cdot o.emb. \quad (3)$$

Spatial Relevance Learning. To fit the real-world scenario described in Section III-B, it is essential to assign higher spatial relevance to nearby objects and lower spatial relevance to distant objects. Therefore, we propose a novel learning-based spatial relevance module to better capture spatial relevance, where $S_{in} = 1 - SDist(q.loc, o.loc)$ is taken as input.

The user’s preference for geo-textual objects increases as the distance decreases and exhibits a stepwise decline as the distance increases, i.e., users tend to visit nearby objects and become less tolerant as the distance increases. To illustrate this stepwise pattern, let us consider a scenario in which a customer wishes to purchase coffee from Starbucks. If the nearest Starbucks is very close, s/he would go and buy coffee. If the nearest Starbucks is a little far, s/he may hesitate and her/his intention of visiting the Starbucks would decrease. If the nearest Starbucks is very far away, s/he would give up this idea. Therefore, a new spatial relevance module is designed, which is a learnable monotonically increasing step function, to align with this real-world characteristic.

Our learning-based spatial relevance module consists of a threshold array $\mathcal{T} \in \mathbb{R}^{t \times 1}$ and a learnable weight array $w_s \in \mathbb{R}^{1 \times t}$. Here, \mathcal{T} is used to ensure that the learned function is a step function and w_s is employed to learn and estimate the spatial relevance. Specifically, \mathcal{T} stores the threshold values that determine the transition points of the step function, i.e., the value exceeded by S_{in} will trigger an increase of spatial relevance. \mathcal{T} is structured as $\mathcal{T}[i] = \frac{i}{t}$, where $i \in [0, t]$ and t is a hyperparameter to control the increment of the threshold value. For example, when $t = 100$, \mathcal{T} is $[0.0, 0.01, \dots, 0.99, 1.0]$. The learnable weight array w_s determines the extent of the increase when the input S_{in} reaches these threshold values. Note that weights in w_s are learned from the training data. When the input S_{in} exceeds the value of $\mathcal{T}[i]$, then the spatial relevance increases by $act(w_s[i])$, where act is an activation function to ensure $act(w_s[i])$ remain non-negative. This process ensures that the output $SRel$ exhibits a step increase as the input S_{in} increases. The learned spatial relevance is computed as below:

$$SRel(q.loc, o.loc) = act(w_s) \cdot \mathbb{I}(S_{in} \geq \mathcal{T}[i]), \quad (4)$$

where $SRel(q.loc, o.loc)$ is the learned spatial relevance. $\mathbb{I} \in \{0, 1\}^{t \times 1}$ is an indicator array. $\mathbb{I}[i] = 1$ if $S_{in} \geq \mathcal{T}[i]$; otherwise 0. The sum of the step increment is conducted by an inner product between the indicator array $\mathbb{I} \in \{0, 1\}^{t \times 1}$ and the learnable weight after activation $act(w_s) \in \mathbb{R}^{1 \times t}$.

During the query phase, we extract the weights in w_s from the module and store them as an array \hat{w}_s for faster inference.

\hat{w}_s is constructed as $\hat{w}_s[i] = \sum_0^i act(w_s[i])$. When computing the spatial relevance, we get the input S_{in} . Since the threshold value grows uniformly by $\frac{1}{t}$, we can determine the number of threshold values exceeded by the input as $\lfloor S_{in} * t \rfloor$, where $\lfloor \cdot \rfloor$ indicates a floor function and is utilized to truncate a real number to an integer. This also corresponds to the sum of the values of weights, which is the spatial relevance score. This process is formulated as:

$$SRel(q.loc, o.loc) = \hat{w}_s[\lfloor S_{in} * t \rfloor]. \quad (5)$$

Hence, during the query phase, the time complexity of computing spatial relevance is $O(1)$, which is efficient.

Adaptive Weight Learning. The latest study [5] has showed the importance of weight learning in improving ranking effectiveness. We rely on the dual-encoder architecture to obtain embedding of query $q.emb$ to compute textual relevance. In addition, our empirical experiments show that the location embedding technique would introduce additional computational costs. Hence, we employ a simple yet effective manner that directly utilizes an MLP layer to determine an optimal weight based on $q.emb$, formulated as follows:

$$w_{st} = MLP(q.emb), w_{st} \in \mathbb{R}^{1 \times 2}. \quad (6)$$

Similar to the Equation 1, the final relevance score between the query and the object is calculated as:

$$ST(q, o) = w_{st} \cdot [TRel(q.doc, o.doc), SRel(q.loc, o.loc)]^T. \quad (7)$$

Training Strategy. To train our relevance model, we employ the contrastive learning strategy. Given a query q_i , the positive (relevant) geo-textual object o_i^+ is obtained by real-world ground-truth data (detailed in Section V-A). For the negative (irrelevant) geo-textual objects, we choose a subset of hard negative objects for training. Specifically, following previous work [5], for each training query, in each training epoch, we randomly pick b hard negative samples from this set. We optimize the loss function as the negative log-likelihood of the positive object:

$$\begin{aligned} L_{\text{model}}(q_i, o_i^+, o_{i,1}^-, o_{i,2}^-, \dots, o_{i,b}^-) \\ = -\log \frac{e^{ST(q_i, o_i^+)}}{e^{ST(q_i, o_i^+)} + \sum_{j=1}^b e^{ST(q_i, o_{i,j}^-)}}. \end{aligned} \quad (8)$$

In addition, we also utilize the in-batch negatives strategy [59] to further enhance training efficiency.

C. The Proposed Index

Figure 3 illustrates our proposed index, which takes geo-location and textual embeddings as input. It uses a Multi-Layer Perception (MLP) to produce the c -cluster probability distribution and employs training strategies to ensure relevant queries and objects have similar probability distributions.

Feature Construction. We utilize geo-location and textual embedding to construct a consistent input representation for both objects and queries, which is illustrated in Figure 3. The textual embedding $emb \in \mathbb{R}^d$ is a d -dimensional embedding, which is converted from textual content $o.doc$ or $q.doc$ by the trained dual encoder module. The geo-location

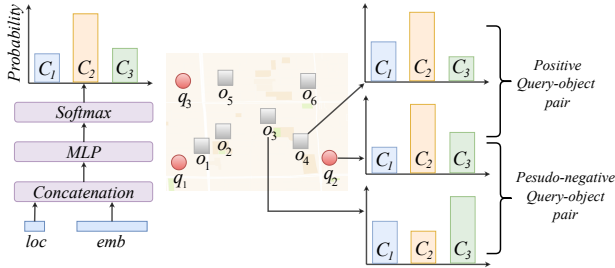


Fig. 3: The illustration of the index.

$loc = \langle lat, lon \rangle$ are transformed into the following features $\langle \hat{lat}, \hat{lon} \rangle$ as below:

$$\hat{lat} = \frac{lat - lat_{min}}{lat_{max} - lat_{min}}, \hat{lon} = \frac{lon - lon_{min}}{lon_{max} - lon_{min}}, \quad (9)$$

where lat_{min} (lon_{min}) represents the lowest latitude (longitude) in dataset D , lat_{max} (lon_{max}) denotes the highest latitude (longitude) in dataset D . Then the input representation is formulated as

$$x = [emb, \hat{lat}, \hat{lon}]. \quad (10)$$

Here x is the input feature vector for the cluster classifier. Although several region embedding techniques exist [60], we find that this simple approach is sufficiently effective. **Cluster Classifier.** Our cluster classifier is a lightweight Multi-Perception Layer (MLP). Given x as the input, it produces the c -cluster probability distribution, defined as follows:

$$Prob = Softmax(MLP(x)), Prob \in [0, 1]^{c \times 1}, \quad (11)$$

where c is a hyperparameter that indicates the desired number of clusters we aim to obtain, and $Prob$ represents the predicted c -cluster probability distribution. The MLP is shared between queries and objects. The c -cluster probability distribution of object o is denoted as $Prob_o$ and that of query q is represented as $Prob_q$. The cluster classifier actually serves as a relevance classifier, grouping identified relevant queries and objects into the same cluster. For example, as illustrated in Figure 3, the object o_4 and query q_2 forms a positive query-object pair, and they are expected to be grouped into the same cluster C_2 .

Pseudo-Label Generation. To train the cluster classifier, both positive and negative pairwise labels are required. We utilize the ground-truth query-object relevant label as the positive pairwise label for training. However, we lack high-quality negative pairwise labels. Randomly selecting negative objects will lead to overfitting and all objects are grouped together (as detailed later). Therefore, we propose a novel pseudo pairwise negative label generation method.

The relationship between query q and object o is denoted as $s(q, o)$. If q and o are relevant, $s(q, o) = 1$; otherwise, $s(q, o) = 0$, which are then used as labels for training. We leverage ground-truth positive labels as pairwise positive labels in the training, as shown below:

$$pos_q = \{o; o \in D, s(q, o) = 1\}, \quad (12)$$

where the positive object set of query q is denoted as pos_q .

The negative object set neg_q of query q is generated by the relevance model. Given a query q , we employ the relevance model to calculate the relevance score for all objects. Then

we adaptively select neg_q according to two hyperparameters neg_{start} and neg_{end} , as shown below:

$$neg_q = \text{argsort}_{o \in D} ST(q, o)[neg_{start} : neg_{end}], s(q, o) = 0, \quad (13)$$

where $ST(q, o)$ is the relevance score between query q and object o produced by the relevance model. Note that positive query-object pairs are excluded as indicated by the filter condition $s(q, o) = 0$.

This adaptive pseudo-negative generation method draws inspiration from hard negative sample strategy [44], [61]. What sets our approach apart from existing studies is that we employ an adaptive manner to select hard negative samples, thereby controlling the difficulty level of the generated negative samples. This adjustment strikes the trade-off between the effectiveness and efficiency.

Decreasing neg_{start} leads to a set of harder negative objects being chosen to train the model. Consequently, the classifier is more effective in distinguishing between positive objects and hard negative objects, which facilitates the clustering of relevant queries and objects, while effectively segregating the irrelevant ones. Empirically, under this setting, only the very relevant queries and objects are grouped into the same cluster. The reduced number of objects within a query's cluster leads to higher efficiency. In contrast, when using a large neg_{start} , the index can not learn useful information, leading to a scenario where all objects tend to be clustered together.

On the other hand, when our index is trained on a set of harder negative objects, it might also exclude some positive ones and reduce its effectiveness. Thus, the choice of neg_{start} strikes a trade-off between effectiveness and efficiency. This alleviates the lack of negative label issue and the skewed cluster distribution issue of existing techniques [18], [19].

Training Strategy. Based on the hard negative objects and positive objects provided above, we employ the MCL loss function [62] to train the MLP, as described below:

$$L_{Index}(q_i, o_i^+, o_{i,1}^-, o_{i,2}^-, \dots, o_{i,m}^-) = \log(\hat{s}(q_i, o_i^+)) + \sum_{j=1}^m \log(1 - \hat{s}(q_i, o_{i,j}^-)), \quad (14)$$

where $\hat{s}(q_i, o_j) = Prob_{q_i}^T \cdot Prob_{o_j}$, $o_i^+ \in pos_q$ and $o_{i,j}^- \in neg_q$. Typically, we randomly select one positive object o_i^+ from the positive object set pos_q and m negative objects from the negative object set neg_q in each training epoch.

As we aim at grouping the relevant pairs of query and object into the same cluster while the irrelevant pairs are into distinct clusters, the queries and objects are jointly incorporated. This is because the MLP is shared between objects and queries. In this manner, the complex relationships between queries and objects can be well learned in the process of index construction. Figure 3 also demonstrates this process, where relevant pairs share similar output and irrelevant ones have different output.

Learning to Partition and Route. During the indexing phase, each object o is partitioned to the cluster with the highest probability according to $Prob_o$. Once the partitioning is completed, the objects assigned to a cluster are stored in a corresponding list, which can act as an inverted file for these objects. Each object in this list is represented by a d -dimensional vector $o.emb$, and a geo-location $o.loc$, which

are utilized to calculate the relevance score for incoming queries. During the query phase, a given query q is directed to the cluster that has the highest probability. Subsequently, the relevance scores between q and all objects in the cluster are calculated and the top- k objects are selected as result objects.

An alternative way is routing queries (objects) to cr clusters with the highest probabilities based on $Prob_q$ ($Prob_o$). Although this might boost query effectiveness by considering more objects in different clusters, it sacrifices efficiency as more objects need to be calculated for a query, leading to an accuracy-efficiency trade-off.

Insertion and Deletion Policy. When a new object comes, we convert it into an embedding using the trained relevance model and then assign it to specific clusters using the trained index. When an object is deleted, we simply remove it from the corresponding cluster. Note that most existing ANNS indexes are static [16], [17], [48]. When inserted data significantly differs in distribution from the existing data or when insertions occur frequently, periodically rebuilding the index is necessary to maintain high accuracy. Our index follows this approach. Apparently, the time costs of insertion and deletion operations are negligible.

Cluster Evaluation. After the training phase, we employ the trained index to produce clusters $C = \{C_1, C_2, \dots, C_c\}$, where C_i represents cluster i . We use validation queries to evaluate the quality of the clusters. The validation queries are fed into the trained index and routed to a cluster. C_i^q denotes a list containing the validation queries routed to C_i , C_i^o denotes a list containing objects partitioned to C_i , and $||$ indicates the size of a list. We proceed to introduce two metrics to evaluate the quality of the clusters.

The first metric evaluates the precision of C_i , denoted as $P(C_i)$, representing the degree to which queries are aligned with their corresponding positive (relevant) objects in the same cluster, which is defined below:

$$P(C_i) = \frac{1}{|C_i^q|} \sum_{q_j \in C_i^q} \frac{|\text{pos}_{q_j} \cap C_i^o|}{|\text{pos}_{q_j}|}. \quad (15)$$

Building upon this, we compute the average precision across all clusters, denoted as $P(C)$, which is defined as below:

$$P(C) = \frac{1}{\sum_{C_i \in C} |C_i^q|} \sum_{C_i \in C} P(C_i) * |C_i^q|. \quad (16)$$

Intuitively, a higher $P(C)$ indicates that the index is more effective.

In addition, we also consider concerns of efficiency. For this purpose, we introduce another metric, the Imbalance Factor (IF) [63], which measures the degree of balance across all clusters, denoted as $IF(C)$. The $IF(C)$ is formulated as:

$$IF(C) = \frac{\sum |C_i|^2}{(\sum |C_i|)^2}, \quad (17)$$

where $IF(C)$ is minimized when $|C_1| = |C_2| = \dots = |C_c|$ according to the Cauchy-Schwarz Inequality. A higher imbalance factor indicates a more uneven distribution of clusters. When most objects are concentrated in a few large clusters, the imbalance factor increases significantly, which is undesirable for our task. Overall, our goal is to achieve high-quality clustering results characterized by higher $P(C)$ and lower

Algorithm 1: Procedures of LIST.

Input: A geo-textual object dataset D , a relevance model R , an index I , training TkQs set Q_{train} , and incoming TkQs set Q

Output: The response Res_q for each query $q \in Q$

- 1 // **Training Phase:** $Train(Q_{\text{train}}, D, R, I)$
- 2 Train R by Q_{train}, D based on Equation 8;
- 3 Employ R to generate pseudo-labels based on Equation 13;
- 4 Employ pseudo-labels to train I based on Equation 14;
- 5 // **Indexing Phase:** $Indexing(D)$
- 6 **for** $o \in D$ **do**
- 7 Transform $o.doc$ to $o.emb$ based on Equation 2;
- 8 Transform $o.emb, o.loc$ to x_o based on Equation 10;
- 9 Generate $Prob_o$ by MLP based on Equation 11;
- 10 Partition o to cluster C_i based on $Prob_o$;
- 11 // **Query Phase:** $Search(q, C, R, I)$
- 12 **for** $q \in Q$ **do**
- 13 Transform $q.doc$ to $q.emb$ based on Equation 2;
- 14 Transform $q.emb, q.loc$ to x_q based on Equation 10;
- 15 Generate $Prob_q$ by I based on Equation 11;
- 16 Route q to cluster C_i based on $Prob_q$;
- 17 $Res_q \leftarrow \text{argTop-}k_{o \in C_i} ST(q, o)$;
- 18 **return** Res_q ;

$IF(C)$. In our index, with proper hyperparameters, our training process of the cluster classifier is able to obtain high-quality clusters. In the experiments, We study the quality of the clusters produced by our proposed index using these evaluation metrics (shown in Section V-E).

D. Procedures and Analyses of LIST

Procedures of LIST. The detailed procedures of LIST are summarized at Algorithm 1. In the training phase, we train the proposed relevance model and index (lines 2-4). After that, in the indexing phase, we assign all objects to their corresponding clusters as inverted files (lines 6-10). In the query phase, given a new query q , we extract its features and then route it to a cluster C_i by the index (lines 13-16). Consequently, we calculate the relevance score between q and each object o in that cluster by the relevance model, and the top- k objects with the highest scores are returned to answer query q (lines 17-18).

Complexity Analysis. Now we analyze the time and space complexity of LIST. Assuming the dimensionality of the embedding is d , the total number of objects is n , and the number of layers in the MLP of the index is l . The embeddings $o.emb$ of objects are generated in advance.

For a given query, the time complexity of LIST is $O((l-2)d^2 + dc + \frac{n}{c}(d+2) + d)$. $O((l-2)d^2 + dc)$ is the time complexity for our index (lines 15), which is the inference computation cost of Equation 11. $O(\frac{n}{c}(d+2) + d)$ is the time cost of our relevance model (line 17). $\frac{n}{c}$ denotes the number of objects to be checked by the relevance model, which is approximately $\frac{1}{c}$ of the entire dataset. This is because of the even cluster distribution (Verified in Section V-E), which means approximately $\frac{1}{c}$ of the dataset needs to be visited. Specifically, $O(\frac{nd}{c})$ is the computational cost of Equation 3. $O(\frac{2n}{c})$ is the computational cost of Equation 5, and $O(d)$ is the computational cost of Equation 6.

The space complexity of LIST is $O((l-1)d + dc) + n(d+2)$. $O((l-1)d + dc)$ is the size of the MLP used by our index.

TABLE I: Datasets Statistics.

| | Beijing | Shanghai | Geo-Glue |
|-------------------------|---------|----------|-----------|
| Number of Pois | 122,420 | 116,859 | 2,849,754 |
| Number of Queries | 168,998 | 127,183 | 90,000 |
| Number of Records | 233,343 | 182,634 | 90,000 |
| Number of Train Queries | 136,890 | 103,019 | 50,000 |
| Number of Val Queries | 15,209 | 11,446 | 20,000 |
| Number of Test Queries | 16,899 | 12,718 | 20,000 |
| Number of Train Records | 189,027 | 148,017 | 50,000 |
| Number of Val Records | 21,034 | 16,492 | 20,000 |
| Number of Test Records | 23,282 | 18,125 | 20,000 |

$O(nd)$ represents the space required for storing pre-computed $o.emb$, and $O(2n)$ denotes the storage cost for geo-locations.

V. EXPERIMENTS

We evaluate the effectiveness and efficiency of our proposed solution in answering TkQs by comparing with state-of-the-art methods on three real-world datasets. We aim to answer the following research questions:

- **RQ1:** Does our proposed retriever LIST and our proposed relevance model outperform previous state-of-the-art methods in terms of effectiveness?
- **RQ2:** How well does the efficiency of our proposed retriever LIST compare with state-of-the-art methods?
- **RQ3:** How does LIST perform on datasets and training datasets of varying sizes?
- **RQ4:** What are the impacts of our proposed index and different modules in the proposed LIST?

A. Experimental Setup

Datasets. We utilize three benchmark datasets: Beijing, Shanghai, and Geo-Glue. The Beijing and Shanghai datasets [5] are provided by Meituan, a Chinese retail services platform. Users submit queries consisting of location and keywords. The clicked Points of Interest (POIs) recorded in the query log are regarded as the ground truth answers to these queries. Note that the click-through data recorded in the search log is widely used as ground-truth for information retrieval evaluation as explicit feedback such as ratings is challenging to collect and implicit feedback such as click-through data can be tracked automatically and is thus much easier to collect for content providers [64]. Both datasets are anonymized to protect user privacy and more details can be found here [5]. The Geo-Glue dataset [12], [65] is released by DAMO Academic. The POIs in the dataset are crawled from OpenStreetMap¹, and the queries and the corresponding ground truth POIs are manually generated by domain experts. Notably, in the released Geo-Glue dataset, the coordinates of objects and queries are modified due to privacy considerations, which results in many objects with identical geo-locations.

Note that, due to privacy considerations, the release of query log datasets from the industry is restricted. *As a result, to our knowledge, no other datasets containing ground-truth query results have been released, except for the three datasets used in our experiment.* To investigate the scalability of the proposed framework, we conduct a scalability study to show LIST’s efficiency on larger datasets, where the Geo-Glue dataset is augmented with more crawled POIs (shown in Section V-D)

Dataset Split. The statistics of datasets are stated in Table I, where each record represents a single ground-truth label between an object and a query, and each query may have multiple ground-truth objects. For the Beijing and Shanghai datasets, to ensure a fair comparison, we follow the previous split strategy [5], where 90% of queries and their corresponding ground-truth records are used as the training set and the remaining queries as the test set. From the training set, we randomly choose 10% data as the validation set to tune hyperparameters. For the Geo-Glue dataset [12], we follow the provided splits for training, validation, and test data.

Effectiveness metric. Following previous studies [5], [12], we use two metrics, i.e., the Recall and Normalized Discounted Cumulative Gain (NDCG), to evaluate the effectiveness. Recall@ k evaluates the proportion of positive objects contained in the top- k candidates for a given query. NDCG@ k considers the order of ground-truth objects in the retrieved objects, reflecting the quality of the ranking in the retrieved list. We assign the graded relevance of the result at position i as $rel_i \in \{0, 1\}$, where $rel_i = 1$ when the object is relevant to the query, otherwise $rel_i = 0$. More details can be found in [5]. Specifically, the following metrics are utilized: Recall@10, Recall@20, NDCG@1, and NDCG@5.

Baselines of Relevance Model. We compare our proposed relevance model, denoted as LIST-R, with various state-of-the-art spatio-textual relevance models or state-of-the-art deep textual relevance models. We also modify the state-of-the-art textual relevance model DPR [38] into DPR_D to answer TkQs.

- TkQ [2]: It uses a traditional relevance model BM25 to evaluate text relevance and utilizes $1-SDist(q.loc, o.loc)$ as spatial relevance. The weight parameter α is manually tuned from 0 to 1 with a footstep of 0.1, and the best effectiveness is achieved when $\alpha = 0.4$ for all three datasets.
- PALM [13]: This method employs deep neural networks for query-object spatio-textual relevance.
- DrW [5]: This is the newest deep relevance based method for answering TkQs.
- DPR [38]: This is a state-of-the-art textual relevance model for document retrieval. This method does not consider spatial relevance.
- DPR_D: This method extends DPR for addressing the TkQs, which employs DPR to calculate textual relevance and uses $1-SDist(q.loc, o.loc)$ as spatial relevance. The weight is learned using the attention mechanism proposed by DrW.
- MGeo [12]: This is also the newest deep relevance based method for answering TkQs. Note that we cannot reproduce the experimental results reported in the paper, and therefore we use the evaluation results from the original paper.

Baselines of LIST. We compare LIST with the following retrieve and rerank methods. We select the IR-Tree [2] to accelerate the TkQ search, serving as an index baseline. There exist two categories of ANNS indexes, as discussed in Section II, and our method belongs to the first category. We select the state-of-the-art ANNS indexes in the first category, i.e., IVF [46], LSH [63], and HNSW [52], as index baselines. For the second category of methods, such as product quantization based methods, their standalone efficiency is no better than a brute-force search². Consequently, following previous work [46], we choose IVFPQ, which integrates PQ with the

¹<https://www.openstreetmap.org/>

²<https://github.com/facebookresearch/faiss/issues/148>

TABLE II: Comparison of relevance models across three datasets by brute-force search.

| | Beijing | | | | Shanghai | | | | Geo-Glue | | | |
|------------------|---------------|---------------|---------------|---------------|---------------|---------------|---------------|---------------|---------------|---------------|---------------|---------------|
| | Recall | | NDCG | | Recall | | NDCG | | Recall | | NDCG | |
| | @20 | @10 | @5 | @1 | @20 | @10 | @5 | @1 | @20 | @10 | @5 | @1 |
| TkQ | 0.5740 | 0.5283 | 0.4111 | 0.3302 | 0.6746 | 0.6380 | 0.5044 | 0.4009 | 0.5423 | 0.5023 | 0.3847 | 0.3051 |
| PALM | 0.3514 | 0.3098 | 0.2077 | 0.1343 | 0.4617 | 0.4023 | 0.2065 | 0.1223 | N/A | N/A | N/A | N/A |
| DrW | 0.6968 | 0.6316 | 0.4814 | 0.3791 | 0.7689 | 0.7159 | 0.5394 | 0.4114 | N/A | N/A | N/A | N/A |
| DPR | 0.5078 | 0.4269 | 0.2892 | 0.2209 | 0.5143 | 0.4161 | 0.2505 | 0.1721 | 0.7626 | 0.7249 | 0.6014 | 0.5079 |
| DPR _D | <u>0.7555</u> | <u>0.6845</u> | <u>0.5181</u> | <u>0.4215</u> | <u>0.7986</u> | <u>0.7494</u> | <u>0.5769</u> | <u>0.4568</u> | <u>0.7963</u> | <u>0.7565</u> | <u>0.6211</u> | <u>0.5202</u> |
| MGeo | N/A | 0.7049 | N/A | N/A | <u>0.5270</u> |
| LIST-R | 0.8156 | 0.7545 | 0.5913 | 0.4989 | 0.8361 | 0.7924 | 0.6445 | 0.5397 | 0.8393 | 0.8033 | 0.6837 | 0.5887 |
| (Gain) | 7.95% | 10.22% | 14.12% | 18.36% | 4.69% | 5.73% | 11.71% | 18.14% | 5.73% | 6.18% | 6.26% | 11.70% |

IVF index from the first category, which is considered as a state-of-the-art solution. Additionally, existing ANNS indexes consider only textual embedding but not the spatial factor. To integrate the spatial factor, we use DPR_D, which is the most effective baseline of the spatio-textual relevance model, to rerank the objects retrieved by an index.

An important hyperparameter is k , which represents the number of objects retrieved by the indexes and reranks by the DPR_D. Specifically, on the Beijing and Shanghai datasets, for a fair comparison, we set k to be 10,000, which is the average number of objects retrieved by our index per query. On the geo-glue dataset, k is set to be 55,000 for the same reason above. We evaluate the effect of k in Section V-C.

- TkQ+DPR_D: This method employs TkQ to retrieve top- k objects and then reranks these objects by DPR_D.
- IVF+DPR_D: This method constructs an IVF index over the embeddings produced by DPR_D, and the objects within the selected index cluster are reranked by DPR_D. Notably, this method requires two parameters: the number of clusters c , and the number of clusters to route for each query and object cr . It does not involve k . We set c and cr to be the same as our method across three datasets for a fair comparison.
- LSH+DPR_D: This method constructs an LSH index with the embeddings produced by the DPR_D, which retrieves the top- k relevant objects by fetching similar embeddings in the same buckets, and reranks the retrieved objects by the DPR_D. Following previous work [63], we set the length of the hash code $nbits$ to 128.
- HNSW+DPR_D: This method constructs an HNSW index over the embeddings produced by the DPR_D, which retrieves the top- k relevant objects by conducting beam searches over the proximity graph, and reranks the retrieved objects by the DPR_D. Following previous work [52], we set the number of links M to 48 and $efConstruction$ to 100.
- IVFPQ+DPR_D: This method integrates the IVF index with the product quantization technique [46] to retrieve objects. The retrieved objects are reranked by the DPR_D. We set the number of clusters c to be the same as our index. Following the instruction [63], we set the number of centroids w to 32 and the number of bits $nbits$ to 8, the number of clusters to search cr at 4. Here, we do not set cr the same as our index since the product quantization accelerates computations within clusters, allowing access to more clusters with comparable time costs. Notably, the maximal k supported by the Faiss library is 2,048, therefore we set k to 2,048 across three datasets.

Due to the page limitation, we demonstrate the effect of key parameters for all these indexes in our full version paper³.

Implementations. The relevance model and the index are trained using Pytorch. During the query phase, the index and all relevance models are inferred in C++ by the ONNX system⁴. In our model, we utilize the bert-base-Chinese pre-trained model⁵ from the huggingface Library [66] as encoders, which is the same as previous work [5], [12]. The footstep controller t of \mathcal{T} is set to be 1000 for all three datasets. neg_{start} is set to 50,000 for the Beijing dataset, 60,000 for the Shanghai dataset, and 200,000 for the Geo-Glue dataset. We empirically set the cluster number c to approximately $\frac{n}{10,000}$, i.e., 20 for the Beijing and Shanghai datasets and 300 for the Geo-Glue dataset. This is because ranking 10,000 objects by the relevance model is computationally feasible and does not notably compromise effectiveness. The number of clusters to route cr for queries and objects is set to 1 by default, with different cr and c settings shown in Section V-C. The implementations of DrW are from publicly available source codes, and we make use of the implementation of IVF, LSH, IVFPQ, and HNSW provided by the Faiss library [63], while others are implemented by ourselves. The Faiss library is implemented in C++, providing a fair comparison with our index. Our default experiment environment is CPU: Intel(R) Core(TM) i9-10900X CPU@3.70GHz, Memory: 128G, and GPU: RTX3080 10GB.

B. Effectiveness Study (RQ1)

Effectiveness of Relevance Model LIST-R. To validate our proposed relevance model’s effectiveness, denoted as LIST-R, we compare it with other relevance models across the three datasets. All relevance models perform a brute-force search over the entire dataset to identify the top- k objects. Table II reports the effectiveness of the evaluated methods. DrW and PLAM cannot be evaluated on the Geo-Glue dataset via brute-force search because of their slow querying speed, requiring more than a day for evaluation. We have the following findings: (1) LIST-R consistently outperforms all the baseline models on all three datasets across every metric. Specifically, LIST-R achieves up to a 19.21% improvement over the best baseline on NDCG@1 and up to a 12.79% improvement on recall@10. (2) Traditional ranking methods are less effective than deep relevance models. On the three datasets, TkQ is

³<https://github.com/Heisenberg-Yin/LIST>

⁴<https://github.com/onnx/onnx>

⁵<https://huggingface.co/bert-base-chinese>

TABLE III: Comparison of retrievers across three datasets.

| | Beijing | | | | Shanghai | | | | Geo-Glue | | | |
|------------------------|---------------|---------------|---------------|---------------|---------------|---------------|---------------|---------------|---------------|---------------|---------------|---------------|
| | Recall | | NDCG | | Recall | | NDCG | | Recall | | NDCG | |
| | @20 | @10 | @5 | @1 | @20 | @10 | @5 | @1 | @20 | @10 | @5 | @1 |
| TkQ+DPR _D | 0.7263 | 0.6633 | 0.5056 | 0.4145 | 0.7717 | 0.7348 | 0.5742 | 0.4556 | 0.7357 | 0.7012 | 0.5797 | 0.4878 |
| IVF+DPR _D | 0.5461 | 0.4954 | 0.3771 | 0.3103 | 0.4965 | 0.4717 | 0.3713 | 0.3000 | 0.4720 | 0.4535 | 0.3835 | 0.3274 |
| LSH+DPR _D | 0.5473 | 0.5057 | 0.3973 | 0.3385 | 0.5356 | 0.5097 | 0.4135 | 0.3453 | 0.6686 | 0.6433 | 0.5445 | 0.4661 |
| HNSW+DPR _D | 0.6267 | 0.5828 | 0.4545 | 0.3765 | 0.5527 | 0.5270 | 0.4182 | 0.3432 | 0.5009 | 0.4807 | 0.4066 | 0.3468 |
| IVFPQ+DPR _D | 0.7064 | 0.6400 | 0.4872 | 0.4002 | 0.7184 | 0.6765 | 0.5257 | 0.4188 | 0.6997 | 0.6724 | 0.5650 | 0.4791 |
| LIST | 0.7711 | 0.7170 | 0.5668 | 0.4812 | 0.7721 | 0.7401 | 0.6099 | 0.5139 | 0.8250 | 0.7909 | 0.6747 | 0.5815 |
| (Gain) | 5.63% | 7.95% | 10.70% | 15.32% | 0.05% | 0.72% | 6.21% | 12.54% | 12.13% | 12.79% | 16.38% | 19.21% |

outperformed by DrW and DPR_D. This can be attributed to the word mismatch issue discussed in Section III-B. Notably, PALM is outperformed by the TkQ, which is consistent with the results reported by [5]. (3) Directly applying the dual-encoder model to our task is less effective. On the Beijing and Shanghai datasets, DPR is outperformed by TkQ, which is caused by the ignorance of spatial relevance. DPR’s enhanced effectiveness on the geo-glue dataset can be attributed to the property of the dataset, where most queries are address descriptions [12].

Effectiveness of LIST. We investigate the effectiveness of LIST by comparing it with the state-of-the-art baselines. The evaluation results are reported in Table III. We have the following findings: (1) Directly applying ANNS indexes in TkQ task results in severe effectiveness degradation. These inferior results can be attributed to the ignorance of the spatial factor by these ANNS indexes. Compared with other ANNS indexes-based methods, TkQ+DPR_D offers better effectiveness across the three datasets. (2) Overall, LIST significantly outperforms all the baselines, achieving the highest scores on all datasets. Compared with the strongest baseline TkQ+DPR_D, LIST achieves up to 12.13% improvements on Recall@10 metric and 19.20% on NDCG@1 metric.

TABLE IV: Query runtime on three datasets (ms).

| | Beijing | Shanghai | Geo-Glue |
|------------------------|------------|------------|------------|
| TkQ | 6.3 | 6.5 | 1,178.0 |
| TkQ+DPR _D | 86.3 | 84.9 | 5,412.3 |
| IVF+DPR _D | 2.9 | 2.9 | 4.0 |
| LSH+DPR _D | 5.2 | 5.1 | 31.1 |
| HNSW+DPR _D | 7.3 | 6.5 | 14.6 |
| IVFPQ+DPR _D | 3.6 | 3.7 | 5.2 |
| LIST | 3.0 | 3.0 | 5.1 |

C. Efficiency Study (RQ2)

Runtime of LIST. We investigate the querying speed of LIST by comparing it with the state-of-the-art baselines. During the query phase, our proposed index, IVF, LSH, IVFPQ, and HNSW remain in the GPU, while IR-Tree remains in the memory. The total runtime is computed by calculating the average time cost of 5,000 randomly sampled queries from the test query set. We present the total runtime of different methods in Table IV. Based on the experimental results, we have the following findings: (1) Compared with the most effective baselines, i.e., TkQ+DPR_D, LIST is one order of magnitude faster on the Beijing and Shanghai datasets and three orders of magnitude faster on the Geo-Glue dataset. (2) IVF+DPR_D and IVFPQ+DPR_D have similar runtimes as LIST. However,

their effectiveness is much worse than LIST as stated in Table III. Specifically, compared with the IVFPQ+DPR_D, LIST achieves an improvement of up to 22.70% on the NDCG@1 metric across the three datasets. Compared with the IVF+DPR_D baseline, we observe an improvement of up to 77.61% on the NDCG@1 metric across the three datasets. (3) The TkQ+DPR_D exhibits a significantly slower querying speed than TkQ across three datasets. The reason is that IR-Tree exploits a priority queue, using the bottom object to prune lower-scoring objects. As the queue size (hyperparameter k) increases, the IR-Tree’s pruning ability declines, aligning with previous empirical results [2].

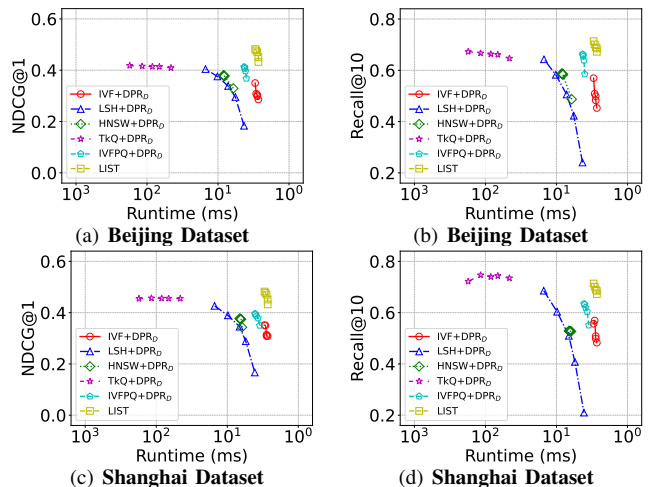


Fig. 4: The Effectiveness-Speed trade-off curve varies with the number of objects retrieved (top- k) and the number of clusters (c) (up and right is better).

Trade-off Study by varying k and c . We examine LIST’s ability to trade off effectiveness and efficiency under the different number of cluster k settings. Specifically, on the Beijing and Shanghai datasets, we set the hyperparameter cluster number c of LIST, IVF+DPR_D, and IVFPQ+DPR_D from 5, 10, 20, 50, to 100. For other baselines, i.e., LSH+DPR_D, HNSW+DPR_D, and TkQ+DPR_D, we set hyperparameter top- k from 40,000, 20,000, 1,0000, 5,000 to 2,000. This ensures the number of objects retrieved for reranking is consistent across different baselines, leading to a fair comparison. Other hyperparameter settings are fixed. We present the trade-off results on the NDCG@1 and Recall@10 metrics for the Beijing and Shanghai datasets in Figure 4 while other metrics and datasets have similar results. We have the following findings: (1) LIST outperforms other methods on both effectiveness and efficiency. This demonstrates LIST’s capability of main-

taining effectiveness while accelerating querying speed. (2) The effectiveness of $\text{TkQ}+\text{DPR}_D$ is consistent as k increases while time overhead increases significantly. This is due to the word mismatch issue discussed in Section III-B. Many relevant objects without word overlap with the query remain hard to retrieve as k increases. (3) $\text{HNSW}+\text{DPR}_D$ exhibits almost constant results. This is because HNSW builds a sparse proximity graph, limiting the reachable objects for each query. Therefore, when k exceeds the number of reachable objects, its performance remains unchanged.

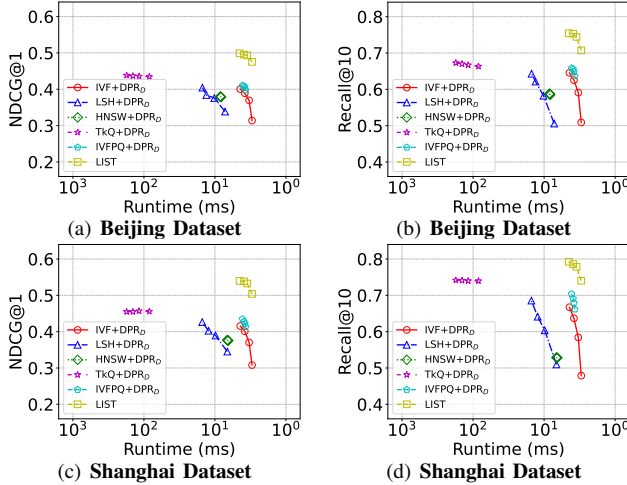


Fig. 5: The Effectiveness-Speed trade-off curve varies with the number of objects retrieved (top- k) and the number of clusters to route (cr) (up and right is better).

Trade-off Study by varying k and cr . We further investigate the impact of the number of clusters cr to route for queries and objects. We vary cr from 1, 2, 3, to 4 for $\text{IVF}+\text{DPR}_D$ and our index, from 4, 5, 6, to 7 for $\text{IVFPQ}+\text{DPR}_D$. For other baselines, we set hyperparameter top- k from 10,000, 20,000, 3,0000, to 4,0000 for a fair comparison like the previous trade-off study. Other hyperparameter settings are fixed. Similarly, we report the trade-off results on $\text{NDCG}@1$ and $\text{Recall}@10$ metrics for the Beijing and Shanghai datasets in Figure 5. According to the experiment results, LIST outperforms other methods in both effectiveness and efficiency under different cr settings. Increasing cr can enhance effectiveness, but it also leads to higher latency. In practice, users can adjust this parameter according to their needs.

Memory Consumption of LIST. The memory consumption of LIST is composed of three parts: the memory used by the proposed relevance model, the memory used by the proposed index, and the memory used for object text embeddings that are produced in advance. The experiment results are presented in Table V, which demonstrates the remarkable memory efficiency of LIST. Compared with $\text{LSH}+\text{DPR}_D$, $\text{TkQ}+\text{DPR}_D$, and $\text{HNSW}+\text{DPR}_D$, LIST requires less memory. The reason is that our index stores only a lightweight MLP c -cluster classifier. This storage requirement is less than the memory consumption of the proximity graph of HNSW, hash tables of LSH, and the inverted file of the IR-Tree.

D. Effect of Dataset Size (RQ3)

Scalability Study. We further explore the scalability of LIST and the proposed relevance model LIST-R. We supplement the Geo-Glue dataset with new POIs crawled from Open Street

TABLE V: Memory usage on three datasets (MB).

| | Beijing | Shanghai | Geo-Glue |
|-----------------------------|---------|----------|----------|
| $\text{TkQ}+\text{DPR}_D$ | 719 | 857 | 12,037 |
| $\text{IVF}+\text{DPR}_D$ | 508 | 505 | 8,510 |
| $\text{LSH}+\text{DPR}_D$ | 513 | 511 | 8,638 |
| $\text{HNSW}+\text{DPR}_D$ | 548 | 545 | 9,427 |
| $\text{IVFPQ}+\text{DPR}_D$ | 508 | 505 | 8,520 |
| LIST | 508 | 505 | 8,515 |

Maps in Hangzhou. For the newly acquired POIs, we utilize the trained dual-encoder module and index to partition them into distinct clusters. We report the runtime of LIST and LIST-R on Figure 6. We observe that, as the number of objects increases, the runtime of LIST and LIST-R scales linearly.

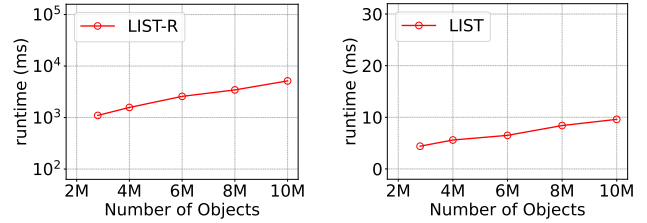


Fig. 6: Scalability study on Geo-Glue dataset.

Effect of Training Dataset Size on Effectiveness. We investigate the impact of training dataset size over LIST and LIST-R. Specifically, we exclude a certain percentage of objects along with their corresponding records during the training and validation process. During testing, we use the complete test dataset. This approach avoids the issue of data leakage. We vary the percentage of objects from 30%, 50%, 80% to 100%. We only present the results for $\text{NDCG}@1$ on the Beijing dataset, as the remaining metrics and datasets have similar results. The results are shown in Figure 7(a). LIST-R uses brute-force search with the relevance model, while LIST utilizes our proposed index for retrieval. The performance gap between them is consistently small, which underscores the capability of our index to boost retrieval speed without sacrificing effectiveness.

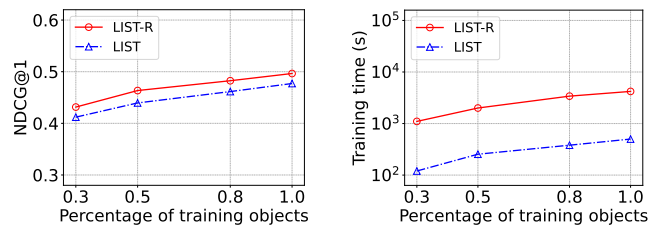


Fig. 7: The impact of training dataset size over effectiveness and training time on Beijing dataset.

In addition, even with low training percentages (e.g., 0.3), our proposed method maintains satisfactory effectiveness, demonstrating its ability to learn from limited data and adapt to new queries.

Effect of Training Dataset Size on Training Time. We also measure the training time per epoch of LIST-R and LIST on the Beijing dataset by varying the size of the training data in the same manner, and the results are shown in Figure 7(b). Other datasets exhibit similar trends. We observe that the training time of LIST-R and LIST appears to be linear to the size of the training data, aligning with our complexity analysis.

E. Ablation Studies (RQ4)

Index Study. To validate the contribution of our proposed index to the overall effectiveness, we compare it with other baseline indexes, including TkQ, IVF, LSH, and HNSW on the Geo-Glue dataset. We employ each index to retrieve objects and then use our proposed relevance model to rerank these objects. The results are reported in Table VI, where all baselines are denoted as Index+LIST-R and use their default hyperparameter settings. We observe that (1) Compared with the IVF+LIST-R, which has comparative querying speed with LIST (Table IV), LIST obtains a 52.33% improvement on the recall@10 metric and 46.84% improvement on the NDCG@1. (2) Our proposed index consistently outperforms other index baselines and delivers at least an order of magnitude faster querying speed. The runtime of Index+LIST-R is close to the runtime of Index+DPR_D, as reported in Table IV.

TABLE VI: Index ablation study on the Geo-Glue dataset.

| | Recall | | NDCG | |
|-------------|---------------|---------------|---------------|---------------|
| | @20 | @10 | @5 | @1 |
| TkQ+LIST-R | 0.7890 | 0.7585 | 0.6517 | 0.5639 |
| IVF+LIST-R | 0.5381 | 0.5192 | 0.4671 | 0.3960 |
| LSH+LIST-R | 0.7665 | 0.7381 | 0.6378 | 0.5555 |
| HNSW+LIST-R | 0.7527 | 0.7231 | 0.6219 | 0.5390 |
| LIST | 0.8250 | 0.7909 | 0.6747 | 0.5815 |

Cluster Quality Study. To illustrate the quality of produced clusters by our index, we conduct a comparison study. We use the proposed relevance model to generate embeddings and then employ our index (denoted as LIST-I) and IVF index to produce clusters separately. We present the cluster results of $IF(C)$ and $P(C)$ in Table VII, which shows that our index achieves much higher precision and obtains comparative imbalance factors compared with IVF index.

TABLE VII: Comparison of the quality of clusters.

| | Beijing | | Shanghai | |
|--------|---------|--------|----------|--------|
| | $IF(C)$ | $P(C)$ | $IF(C)$ | $P(C)$ |
| IVF | 1.31 | 0.6774 | 1.33 | 0.6418 |
| LIST-I | 1.49 | 0.8907 | 1.43 | 0.8382 |

Pseudo-Label Study. As discussed in Section IV-C, the parameter neg_{start} affects the difficulty level of pseudo-negative labels, which then impacts the effectiveness and efficiency of our index. To investigate the impacts of the pseudo-negative labels, we vary the hyperparameter neg_{start} from 40,000, 50,000, 60,000, and 70,000, to 80,000 on the Beijing and Shanghai datasets. We illustrate the metrics $P(C)$ and $IF(C)$ of produced clusters in Figure 8. Notably, as neg_{start} increases, both $IF(C)$ and $P(C)$ tend to increase. An increased $IF(C)$ suggests a more concentrated distribution of objects, while an increased $P(C)$ indicates improved accuracy in the retrieval results. The experiment results indicate that the choice of neg_{start} leads to a trade-off between effectiveness and efficiency, which can be set flexibly in real-world applications.

Spatial Learning Study. To evaluate the learning-based spatial relevance module, we consider the following baseline: (1) LIST-R+ S_{in} that replaces the learning-based spatial relevance module with $S_{in}=1-SDist(q.loc, o.loc)$ for training; and (2) LIST-R+ $\alpha * S_{in}^{\beta}$ which substitutes the spatial relevance

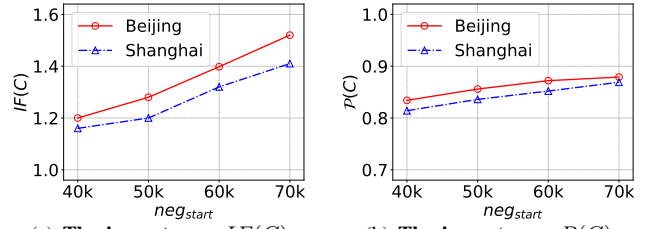


Fig. 8: The impact of neg_{start} over the cluster quality.

module with a learnable exponential function. α and β are two learnable parameters and are processed to ensure non-negative. Table VIII presents the experimental results obtained by conducting a brute-force search on the Beijing dataset using the trained models. Notably, LIST-R outperforms LIST-R+ S_{in} in all metrics. Interestingly, the first variant outperforms the second variant, which suggests that without careful design, a learnable function may be outperformed by a simple approach.

TABLE VIII: Ablation study of spatial relevance module and weight learning via brute-force search on the Beijing dataset.

| | Recall | | NDCG | |
|------------------------------------|---------------|---------------|---------------|---------------|
| | @20 | @10 | @5 | @1 |
| LIST-R + S_{in} | 0.7526 | 0.7087 | 0.5255 | 0.4271 |
| LIST-R + $\alpha * S_{in}^{\beta}$ | 0.5308 | 0.4532 | 0.3130 | 0.2411 |
| LIST-R + ADrW | 0.7925 | 0.7414 | 0.5832 | 0.4792 |
| LIST-R | 0.8156 | 0.7545 | 0.5913 | 0.4989 |

Weight Learning Study. We conduct a comparison experiment between our weight learning module and the attention mechanism proposed by DrW [5] (denoted as ADrW). Table VIII reports the results obtained by conducting a brute-force search on the Beijing dataset using the trained relevance models. Here, LIST-R represents our weight learning mechanism, while LIST-R+ADrW denotes replacing it with the ADrW for training. The results indicate that our weight learning mechanism surpasses the latest ADrW mechanism.

VI. CONCLUSIONS AND FUTURE WORK

In this paper, we propose a novel retriever LIST, which comprises a new relevance model and a novel index. We conduct extensive experiments to show the effectiveness and efficiency of LIST over the state-of-the-art baselines. This work opens up a promising research direction of designing novel ANNS indexes for accelerating the search for embedding based spatial keyword queries. One interesting future direction is integrating our index with product quantization techniques to further expedite the search process. Another potential direction is to extend our proposed index to vector databases for dense vectors without spatial information.

REFERENCES

- [1] Y. Chen, X. Li, G. Cong, C. Long, Z. Bao, S. Liu, W. Gu, and F. Zhang, "Points-of-interest relationship inference with spatial-enriched graph neural networks," *Proceedings of the VLDB Endowment*, vol. 15, no. 3, pp. 504–512, 2021.
- [2] G. Cong, C. S. Jensen, and D. Wu, "Efficient retrieval of the top-k most relevant spatial web objects," *Proceedings of the VLDB Endowment*, vol. 2, no. 1, pp. 337–348, 2009.
- [3] Y. Chen, T. Suel, and A. Markowetz, "Efficient query processing in geographic web search engines," in *Proceedings of the ACM SIGMOD International Conference on Management of Data, Chicago, Illinois, USA, June 27-29, 2006*. ACM, 2006, pp. 277–288.

- [4] A. Cary, O. Wolfson, and N. Rische, "Efficient and scalable method for processing top-k spatial boolean queries," in *Scientific and Statistical Database Management, 22nd International Conference, SSDBM 2010, Heidelberg, Germany, June 30 - July 2, 2010. Proceedings*, ser. Lecture Notes in Computer Science, vol. 6187. Springer, 2010, pp. 87–95.
- [5] S. Liu, G. Cong, K. Feng, W. Gu, and F. Zhang, "Effectiveness perspectives and a deep relevance model for spatial keyword queries," *Proceedings of the ACM on Management of Data*, vol. 1, no. 1, pp. 1–25, 2023.
- [6] Z. Chen, L. Chen, G. Cong, and C. S. Jensen, "Location- and keyword-based querying of geo-textual data: a survey," *VLDB J.*, vol. 30, no. 4, pp. 603–640, 2021.
- [7] I. D. Felipe, V. Hristidis, and N. Rische, "Keyword search on spatial databases," in *Proceedings of the 24th International Conference on Data Engineering, ICDE 2008, April 7-12, 2008, Cancún, Mexico*. IEEE Computer Society, 2008, pp. 656–665.
- [8] Z. Li, K. C. K. Lee, B. Zheng, W. Lee, D. L. Lee, and X. Wang, "Irtree: An efficient index for geographic document search," *IEEE Trans. Knowl. Data Eng.*, vol. 23, no. 4, pp. 585–599, 2011.
- [9] J. B. Rocha-Junior, O. Gkorgkas, S. Jonassen, and K. Nørnvåg, "Efficient processing of top-k spatial keyword queries," in *Advances in Spatial and Temporal Databases - 12th International Symposium, SSTD 2011, Minneapolis, MN, USA, August 24-26, 2011, Proceedings*, ser. Lecture Notes in Computer Science, vol. 6849. Springer, 2011, pp. 205–222.
- [10] S. E. Robertson and H. Zaragoza, "The probabilistic relevance framework: BM25 and beyond," *Found. Trends Inf. Retr.*, vol. 3, no. 4, pp. 333–389, 2009.
- [11] H. C. Wu, R. W. P. Luk, K. Wong, and K. Kwok, "Interpreting TF-IDF term weights as making relevance decisions," *ACM Trans. Inf. Syst.*, vol. 26, no. 3, pp. 13:1–13:37, 2008.
- [12] R. Ding, B. Chen, P. Xie, F. Huang, X. Li, Q. Zhang, and Y. Xu, "Mgeo: Multi-modal geographic language model pre-training," in *Proceedings of the 46th International ACM SIGIR Conference on Research and Development in Information Retrieval, SIGIR 2023, Taipei, Taiwan, July 23-27, 2023*, H.-H. Chen, W.-J. E. Duh, H.-H. Huang, M. P. Kato, J. Mothe, and B. Poblete, Eds. ACM, 2023, pp. 185–194.
- [13] J. Zhao, D. Peng, C. Wu, H. Chen, M. Yu, W. Zheng, L. Ma, H. Chai, J. Ye, and X. Qie, "Incorporating semantic similarity with geographic correlation for query-poi relevance learning," in *The Thirty-Third AAAI Conference on Artificial Intelligence, AAAI 2019, Honolulu, Hawaii, USA, January 27 - February 1, 2019*. AAAI Press, 2019, pp. 1270–1277.
- [14] N. Beckmann, H. Kriegel, R. Schneider, and B. Seeger, "The r*-tree: An efficient and robust access method for points and rectangles," in *Proceedings of the 1990 ACM SIGMOD International Conference on Management of Data, Atlantic City, NJ, USA, May 23-25, 1990*. ACM Press, 1990, pp. 322–331.
- [15] J. Qin, W. Wang, C. Xiao, Y. Zhang, and Y. Wang, "High-dimensional similarity query processing for data science," in *KDD '21: The 27th ACM SIGKDD Conference on Knowledge Discovery and Data Mining, Virtual Event, Singapore, August 14-18, 2021*. ACM, 2021, pp. 4062–4063.
- [16] J. Wang, T. Zhang, J. Song, N. Sebe, and H. T. Shen, "A survey on learning to hash," *IEEE Trans. Pattern Anal. Mach. Intell.*, vol. 40, no. 4, pp. 769–790, 2018.
- [17] M. Wang, X. Xu, Q. Yue, and Y. Wang, "A comprehensive survey and experimental comparison of graph-based approximate nearest neighbor search," *Proceedings of the VLDB Endowment*, vol. 14, no. 11, pp. 1964–1978, 2021.
- [18] Y.-C. Hsu and Z. Kira, "Neural network-based clustering using pairwise constraints," vol. abs/1511.06321, 2015.
- [19] Y. Hsu, Z. Lv, and Z. Kira, "Learning to cluster in order to transfer across domains and tasks," in *6th International Conference on Learning Representations, ICLR 2018, Vancouver, BC, Canada, April 30 - May 3, 2018, Conference Track Proceedings*. OpenReview.net, 2018.
- [20] C. Zhang, Y. Zhang, W. Zhang, and X. Lin, "Inverted linear quadtree: Efficient top k spatial keyword search," in *29th IEEE International Conference on Data Engineering, ICDE 2013, Brisbane, Australia, April 8-12, 2013*. IEEE Computer Society, 2013, pp. 901–912.
- [21] Y. Tao and C. Sheng, "Fast nearest neighbor search with keywords," *IEEE Trans. Knowl. Data Eng.*, vol. 26, no. 4, pp. 878–888, 2014.
- [22] S. Vaid, C. B. Jones, H. Joho, and M. Sanderson, "Spatio-textual indexing for geographical search on the web," in *Advances in Spatial and Temporal Databases, 9th International Symposium, SSTD 2005, Angra dos Reis, Brazil, August 22-24, 2005, Proceedings*, ser. Lecture Notes in Computer Science, vol. 3633. Springer, 2005, pp. 218–235.
- [23] R. Göbel, A. Henrich, R. Niemann, and D. Blank, "A hybrid index structure for geo-textual searches," in *Proceedings of the 18th ACM Conference on Information and Knowledge Management, CIKM 2009, Hong Kong, China, November 2-6, 2009*. ACM, 2009, pp. 1625–1628.
- [24] Y. Zhou, X. Xie, C. Wang, Y. Gong, and W. Ma, "Hybrid index structures for location-based web search," in *Proceedings of the 2005 ACM CIKM International Conference on Information and Knowledge Management, Bremen, Germany, October 31 - November 5, 2005*. ACM, 2005, pp. 155–162.
- [25] J. Lu, Y. Lu, and G. Cong, "Reverse spatial and textual k nearest neighbor search," in *Proceedings of the ACM SIGMOD International Conference on Management of Data, SIGMOD 2011, Athens, Greece, June 12-16, 2011*. ACM, 2011, pp. 349–360.
- [26] D. Zhang, K. Tan, and A. K. H. Tung, "Scalable top-k spatial keyword search," in *Joint 2013 EDBT/ICDT Conferences, EDBT '13 Proceedings, Genoa, Italy, March 18-22, 2013*. ACM, 2013, pp. 359–370.
- [27] D. Zhang, B. C. Ooi, and A. K. H. Tung, "Locating mapped resources in web 2.0," in *Proceedings of the 26th International Conference on Data Engineering, ICDE 2010, March 1-6, 2010, Long Beach, California, USA*. IEEE Computer Society, 2010, pp. 521–532.
- [28] D. Zhang, Y. M. Chee, A. Mondal, A. K. H. Tung, and M. Kitsuregawa, "Keyword search in spatial databases: Towards searching by document," in *Proceedings of the 25th International Conference on Data Engineering, ICDE 2009, March 29 2009 - April 2 2009, Shanghai, China*. IEEE Computer Society, 2009, pp. 688–699.
- [29] Y. Sheng, X. Cao, Y. Fang, K. Zhao, J. Qi, G. Cong, and W. Zhang, "WISK: A workload-aware learned index for spatial keyword queries," *Proc. ACM Manag. Data*, vol. 1, no. 2, pp. 187:1–187:27, 2023.
- [30] Y. Liu and A. Magdy, "U-ASK: a unified architecture for knn spatial-keyword queries supporting negative keyword predicates," in *Proceedings of the 30th International Conference on Advances in Geographic Information Systems, SIGSPATIAL 2022, Seattle, Washington, November 1-4, 2022*. ACM, 2022, pp. 40:1–40:11.
- [31] Z. Qian, J. Xu, K. Zheng, P. Zhao, and X. Zhou, "Semantic-aware top-k spatial keyword queries," *World Wide Web*, vol. 21, no. 3, pp. 573–594, 2018.
- [32] X. Chen, J. Xu, R. Zhou, P. Zhao, C. Liu, J. Fang, and L. Zhao, "S²-tree: a pivot-based indexing structure for semantic-aware spatial keyword search," *Geoinformatica*, vol. 24, no. 1, pp. 3–25, 2020.
- [33] P. Indyk and R. Motwani, "Approximate nearest neighbors: Towards removing the curse of dimensionality," in *Proceedings of the Thirtieth Annual ACM Symposium on Theory of Computing - STOC '98, 1998*, pp. 604–613.
- [34] J. Guo, Y. Fan, L. Pang, L. Yang, Q. Ai, H. Zamani, C. Wu, W. B. Croft, and X. Cheng, "A deep look into neural ranking models for information retrieval," *Information Processing & Management*, vol. 57, no. 6, p. 102067, 2020.
- [35] B. Hu, Z. Lu, H. Li, and Q. Chen, "Convolutional neural network architectures for matching natural language sentences," in *Advances in Neural Information Processing Systems 27: Annual Conference on Neural Information Processing Systems 2014, December 8-13 2014, Montreal, Quebec, Canada, 2014*, pp. 2042–2050.
- [36] L. Pang, Y. Lan, J. Guo, J. Xu, S. Wan, and X. Cheng, "Text matching as image recognition," in *Proceedings of the Thirtieth AAAI Conference on Artificial Intelligence, February 12-17, 2016, Phoenix, Arizona, USA, 2016*, pp. 2793–2799.
- [37] P.-S. Huang, X. He, J. Gao, L. Deng, A. Acero, and L. Heck, "Learning deep structured semantic models for web search using clickthrough data," in *Proceedings of the 22nd ACM International Conference on Conference on Information & Knowledge Management - CIKM '13, 2013*, pp. 2333–2338.
- [38] V. Karpukhin, B. Oguz, S. Min, P. S. H. Lewis, L. Wu, S. Edunov, D. Chen, and W.-t. Yih, "Dense passage retrieval for open-domain question answering," in *Proceedings of the 2020 Conference on Empirical Methods in Natural Language Processing, EMNLP 2020, Online, November 16-20, 2020, 2020*, pp. 6769–6781.
- [39] K. Guu, K. Lee, Z. Tung, P. Pasupat, and M. Chang, "Retrieval augmented language model pre-training," in *Proceedings of the 37th International Conference on Machine Learning, ICML 2020, 13-18 July 2020, Virtual Event*, ser. Proceedings of Machine Learning Research, vol. 119. PMLR, 2020, pp. 3929–3938.
- [40] J. Guo, Y. Cai, Y. Fan, F. Sun, R. Zhang, and X. Cheng, "Semantic models for the first-stage retrieval: A comprehensive review," *ACM Trans. Inf. Syst.*, vol. 40, no. 4, pp. 66:1–66:42, 2022.
- [41] W. X. Zhao, J. Liu, R. Ren, and J. Wen, "Dense text retrieval based on pretrained language models: A survey," *CoRR*, vol. abs/2211.14876, 2022.
- [42] K. Zhou, X. Liu, Y. Gong, W. X. Zhao, D. Jiang, N. Duan, and J. Wen, "MASTER: multi-task pre-trained bottlenecked masked autoencoders are better dense retrievers," in *Machine Learning and Knowledge Discovery in Databases: Research Track - European Conference, ECML PKDD 2023, Turin, Italy, September 18-22, 2023, Proceedings, Part II*, ser. Lecture Notes in Computer Science, vol. 14170. Springer, 2023, pp. 630–647.

- [43] X. Wen, X. Chen, X. Chen, B. He, and L. Sun, "Offline pseudo relevance feedback for efficient and effective single-pass dense retrieval," in *Proceedings of the 46th International ACM SIGIR Conference on Research and Development in Information Retrieval*, 2023, pp. 2209–2214.
- [44] Y. Qu, Y. Ding, J. Liu, K. Liu, R. Ren, W. X. Zhao, D. Dong, H. Wu, and H. Wang, "Rocketqa: An optimized training approach to dense passage retrieval for open-domain question answering," in *Proceedings of the 2021 Conference of the North American Chapter of the Association for Computational Linguistics: Human Language Technologies, NAACL-HLT 2021, Online, June 6-11, 2021*. Association for Computational Linguistics, 2021, pp. 5835–5847.
- [45] A. Babenko and V. S. Lempitsky, "The inverted multi-index," *IEEE Trans. Pattern Anal. Mach. Intell.*, vol. 37, no. 6, pp. 1247–1260, 2015.
- [46] H. Jégou, M. Douze, and C. Schmid, "Product quantization for nearest neighbor search," *IEEE Transactions on Pattern Analysis and Machine Intelligence*, vol. 33, no. 1, pp. 117–128, 2011.
- [47] R. Wang and D. Deng, "Deltapq: lossless product quantization code compression for high dimensional similarity search," *Proceedings of the VLDB Endowment*, vol. 13, no. 13, pp. 3603–3616, 2020.
- [48] X. Luo, H. Wang, D. Wu, C. Chen, M. Deng, J. Huang, and X.-S. Hua, "A survey on deep hashing methods," *ACM Transactions on Knowledge Discovery from Data*, vol. 17, no. 1, pp. 1–50, 2023.
- [49] Y. Liu, J. Cui, Z. Huang, H. Li, and H. T. Shen, "Sk-lsh: an efficient index structure for approximate nearest neighbor search," *Proceedings of the VLDB Endowment*, vol. 7, no. 9, pp. 745–756, 2014.
- [50] W. Liu, H. Wang, Y. Zhang, W. Wang, and L. Qin, "l-lsh: l/o efficient c-approximate nearest neighbor search in high-dimensional space," in *2019 IEEE 35th International Conference on Data Engineering (ICDE)*. IEEE, 2019, pp. 1670–1673.
- [51] B. Zheng, Z. Xi, L. Weng, N. Q. V. Hung, H. Liu, and C. S. Jensen, "Pm-lsh: A fast and accurate lsh framework for high-dimensional approximate nn search," *Proceedings of the VLDB Endowment*, vol. 13, no. 5, pp. 643–655, 2020.
- [52] Y. A. Malkov and D. A. Yashunin, "Efficient and robust approximate nearest neighbor search using hierarchical navigable small world graphs," *IEEE Transactions on Pattern Analysis and Machine Intelligence*, vol. 42, no. 4, pp. 824–836, 2020.
- [53] J. Wang, H. T. Shen, J. Song, and J. Ji, "Hashing for similarity search: A survey," *CoRR*, vol. abs/1408.2927, 2014.
- [54] T. Ge, K. He, Q. Ke, and J. Sun, "Optimized product quantization," *IEEE Trans. Pattern Anal. Mach. Intell.*, vol. 36, no. 4, pp. 744–755, 2014.
- [55] L. Gao, X. Zhu, J. Song, Z. Zhao, and H. T. Shen, "Beyond product quantization: Deep progressive quantization for image retrieval," in *Proceedings of the Twenty-Eighth International Joint Conference on Artificial Intelligence, IJCAI 2019, Macao, China, August 10-16, 2019*. ijcai.org, 2019, pp. 723–729.
- [56] R. Guo, P. Sun, E. Lindgren, Q. Geng, D. Simcha, F. Chern, and S. Kumar, "Accelerating large-scale inference with anisotropic vector quantization," in *Proceedings of the 37th International Conference on Machine Learning, ICML 2020, 13-18 July 2020, Virtual Event*, ser. Proceedings of Machine Learning Research, vol. 119. PMLR, 2020, pp. 3887–3896.
- [57] Z. Yuan, H. Liu, Y. Liu, D. Zhang, F. Yi, N. Zhu, and H. Xiong, "Spatio-temporal dual graph attention network for query-poi matching," in *Proceedings of the 43rd International ACM SIGIR conference on research and development in Information Retrieval, SIGIR 2020, Virtual Event, China, July 25-30, 2020*. ACM, 2020, pp. 629–638.
- [58] J. Devlin, M. Chang, K. Lee, and K. Toutanova, "BERT: pre-training of deep bidirectional transformers for language understanding," in *Proceedings of the 2019 Conference of the North American Chapter of the Association for Computational Linguistics: Human Language Technologies, NAACL-HLT 2019, Minneapolis, MN, USA, June 2-7, 2019, Volume 1 (Long and Short Papers)*. Association for Computational Linguistics, 2019, pp. 4171–4186.
- [59] S.-C. Lin, J.-H. Yang, and J. Lin, "In-batch negatives for knowledge distillation with tightly-coupled teachers for dense retrieval," in *Proceedings of the 6th Workshop on Representation Learning for NLP (RePLANLP-2021)*. Association for Computational Linguistics, 2021, pp. 163–173.
- [60] D. Paul, F. Li, and J. M. Phillips, "Semantic embedding for regions of interest," *VLDB J.*, vol. 30, no. 3, pp. 311–331, 2021.
- [61] R. Ren, Y. Qu, J. Liu, W. X. Zhao, Q. She, H. Wu, H. Wang, and J. Wen, "Rocketqav2: A joint training method for dense passage retrieval and passage re-ranking," in *Proceedings of the 2021 Conference on Empirical Methods in Natural Language Processing, EMNLP 2021, Virtual Event / Punta Cana, Dominican Republic, 7-11 November, 2021*. Association for Computational Linguistics, 2021, pp. 2825–2835.
- [62] Y. Hsu, Z. Lv, J. Schlosser, P. Odom, and Z. Kira, "Multi-class classification without multi-class labels," in *7th International Conference on Learning Representations, ICLR 2019, New Orleans, LA, USA, May 6-9, 2019*. OpenReview.net, 2019.
- [63] J. Johnson, M. Douze, and H. Jégou, "Billion-scale similarity search with GPUs," *IEEE Transactions on Big Data*, vol. 7, no. 3, pp. 535–547, 2019.
- [64] X. He, L. Liao, H. Zhang, L. Nie, X. Hu, and T. Chua, "Neural collaborative filtering," in *Proceedings of the 26th International Conference on World Wide Web, WWW 2017, Perth, Australia, April 3-7, 2017*. ACM, 2017, pp. 173–182.
- [65] D. Li, R. Ding, Q. Zhang, Z. Li, B. Chen, P. Xie, Y. Xu, X. Li, N. Guo, F. Huang, and X. He, "Geogluce: A geographic language understanding evaluation benchmark," *CoRR*, vol. abs/2305.06545, 2023.
- [66] T. Wolf, L. Debut, V. Sanh, J. Chaumond, C. Delangue, A. Moi, P. Cistac, T. Rault, R. Louf, M. Funtowicz, and J. Brew, "Huggingface's transformers: State-of-the-art natural language processing," *CoRR*, vol. abs/1910.03771, 2019.